Cleaner Engineering and Technology 11 (2022) 100583

Contents lists available at ScienceDirect

Cleaner Engineering and Technology

journal homepage: www.sciencedirect.com/journal/cleaner-engineering-and-technology

Mechanical and durability property dimensions of sustainable bamboo leaf ash in high-performance concrete

David O. Nduka [a,*], Babatunde J. Olawuyi [b], Adekunle M. Ajao [a], Victor C. Okoye [a], Obinna M. Okigbo [a]

[a] Department of Building Technology, College of Science and Technology, Covenant University, Ota, Ogun State, Nigeria
[b] Department of Building, School of Environmental Technology, Federal University of Technology, Minna, Nigeria

ARTICLE INFO

Keywords:
Bamboo leaf ash
High-performance concrete
Superabsorbent polymers
Superplaticiser
Supplementary cementitious materials
Sustainability

ABSTRACT

This research characterises bamboo leaf ash (BLA), which was obtained by calcining dry bamboo leaves at approximately 600 °C for 2 h in a laboratory-controlled muffle furnace. To understand the pozzolanic potentials of the BLA, X-ray fluorescence (XRF) and scanning electron microscope/energy dispersive x-ray (SEM/EDX) techniques were employed. The BLA was then mixed with Portland cement (PC) to produce high-performance concrete (HPC) at 0, 5, 10, and 15% BLA contents by weight. Fresh HPC samples were evaluated for their workability with slump flow test. After 7, 21, 28, and 60 days of hydration, HPC samples' mechanical (compressive, splitting tensile, and flexural) and durability (water absorption, sorptivity, and influence of aggressive environments) were measured. As determined by XRF, the calcined BLA has pozzolanic properties, whereas the SEM micrograph exhibits irregular and angular morphologies. The incorporation of BLA into the HPC matrix enhanced the mechanical and durability qualities of the evaluated samples, primarily at a substitution rate of 10% PC. Therefore, it can be stated that 10% BLA can substitute cement in an HPC subjected to standard environmental conditions.

1. Introduction

The concept of high-strength concrete (HSC)/high-performance concrete (HPC) is fundamental to concrete technology. The significance derives from the precisely chosen ingredients and mixture ratios that are optimally designed to have primarily improved qualities, such as high strength and low permeability (Xu et al., 2021; Dushimimana et al., 2021; Zeyad *et al.*, 2022). The American Concrete Institute, ACI (1999) defined HPC as concrete that satisfies unique performance and uniformity requirements that cannot ordinarily be obtained using standard constituents, a standard blending technique, and curing practices. The desirable features of HPCs include high resistance to abrasion and damage tolerance, long lifespan in harsh environments, resistance to environmental attacks and impacts (Dushimimana et al., 2021) and easy placement (Zeyad et al., 2021a, 2021b). HPC is exclusively used in high-rise buildings, long-span bridges (Nduka et al., 2018; Dushimimana et al., 2021), tunnels, and maritime structures (Odeyemi et al., 2022). According to Mehta and Monteiro (2017), the strength classification suggests that HPC has a compressive strength of at least 50 MPa. The value of 50 MPa was chosen because it corresponds to a level of quality at which much care must be taken while developing and testing concrete. To meet the needs of HPC, a unique design may be necessary, while supplementary cementitious materials (SCMs), also known as pozzolans, contribute significantly to the characteristics.

The addition of industrial (iron slag, copper slag, electrolytic manganese residue, glass waste, lithium slag, and ferro-silica wastes (Zeyad et al., 2021a; Zeyad et al., 2021b) and agricultural (rice husk ash, bamboo leaf ash, palm oil fuel ash, cotton stalk, egg shell powder and olive waste ash etc.) (Odeyemi et al., 2022) based-SCMs in concrete and mortar is one approach to promote sustainable development in the building sector. K Al-Chaar et al. (2013) opine that SCM can substitute a large portion of cement in a concrete mixture with characteristics similar to Portland cement. Dembovska et al. (2017) posit that the amount of portlandite created during cement hydration would decrease related to the amount of SCMs used in a mixture. SCMs are products that are not cementitious in themselves but comprise reactive elements such as silica and alumina in a partitioned structure capable of being mixed with calcium hydroxide once water is present to create mixtures with

* Corresponding author.
E-mail address: david.nduka@covenantuniversity.edu.ng (D.O. Nduka).

https://doi.org/10.1016/j.clet.2022.100583
Received 27 May 2022; Received in revised form 9 October 2022; Accepted 1 November 2022
Available online 5 November 2022

cementitious properties (Silva et al., 2021). SCMs may be in the form of natural (pumice, perlite, volcanic ash and diatomaceous earth) (Kasaniya et al., 2021), agricultural (sugar cane bagasse ash, rice husk ash, sorghum husk ash, coconut shell ash, and bamboo leaf ash) (Mo et al., 2016) and industrial origins (silica fume, fly ash, granulated blast furnace slag (Chinnu et al., 2021; Kasaniya et al., 2021). Irrespective of the SCM sources, their later-age strength characteristics have the potential to improve the mechanical, durability and microstructural performances of mortar and concrete.

Recent attention has been paid to bamboo leaf ash (BLA) as an agricultural waste with pozzolanic reactivity. Bamboo is a renewable resource that may thrive in various environments, particularly in tropical and subtropical nations (Mo et al., 2016). Annual bamboo use by the food, brewing, construction, agricultural, fibre, paper, and board industries is estimated at 20 million tonnes (Kolawole et al., 2021). These industries generate huge amounts of bamboo waste for which alternative applications have not been fully exploited. Frequently, the waste is burned in an open location, resulting in environmental deterioration. Kolawole et al. (2021) calculated that more than 1% of the tropical forest is covered by bamboo. The plantation deposits many dry leaves as agricultural waste beneath them. Activating their pozzolanic reactivity via calcination in a controlled setting is one of the sustainable methods for utilising bamboo leaf waste as an SCM. According to Dwivedia et al. (2006), BLA calcined at a regulated temperature of 600 °C for 2 h will exhibit a significant pozzolanic reactivity. Similar claims were made by Villar-Cociña et al. (2011) and Frías et al. (2012), confirming that calcined ash obtained from bamboo leaf waste is an effective SCM material for producing mortar and concrete. Rodier et al. (2019) investigated the pozzolanic activity and compressive strength of BLA mortar mixes. The mixtures produced a pozzolanic reaction between amorphous silica and lime, forming a calcium silicate hydrate (C-S-H). At 28 days of curing, the compressive strength behaviour of their evaluated samples improved more than the control mix. In addition, Kolawole et al.'s (2021) findings on the investigated PC replacement with BLA revealed that up to 10% BLA content in the cement-based matrix developed over 75% compressive strength as anticipated from a pozzolanic cement at 7 and 28 days of hydration period.

The binary blend of BLA and cement in HPC is underrepresented in the identified research. Most research on BLA in concrete is centred on normal-strength concrete with 20-35 MPa compressive strength, which is marred by degradation concerns (Oyebisi et al., 2020; Nduka et al., 2022). Nevertheless, a more recent work by Odeyemi et al. (2022) demonstrated that 5% PC substitution with BLA in the HPC mixture improved the evaluated samples' mechanical and microstructural properties. In Nigeria, the concrete production quality has been identified as one of the primary causes of the failure and collapse of concrete structures (Kolawole, 2015), with many construction professionals being unaware of SCM utilisation in mortar and concrete works (Nduka et al., 2018). Investigating concrete quality by combining PC and BLA in HPC production would raise awareness among construction professionals regarding new alternative materials in building projects. Therefore, this study investigates the mechanical and durability properties of BLA-blended HPC to establish their appropriateness for structural element works.

2. Materials and method

2.1. Binders and admixtures

The cement used was Dangote "3X" Portland-limestone cement (PC) with the marking "CEM II B-L, 42.5 N" This Portland cement brand conforms to BS EN 197-1 (2011) and NIS 444-1 (2018) requirements. This experiment collected bamboo leaves in Ijo-Ota, Ogun State, Nigeria. The leaves were sun-dried to reduce their moisture content, then calcined in an open drum to an undetermined temperature and allowed to cool to room temperature. The ash was subsequently compressed and calcined at a controlled temperature in the foundry workshop of Covenant University in Ota, Ogun state, using a muffle furnace. Following calcination at 600 °C for approximately 2 h, the ash was air-cooled and further sieved according to Silva et al.'s (2021) BLA thermal treatment methodology. According to Moraes et al. (2019), BLA calcined between 500 °C and 600 °C demonstrated significantly more pozzolanic reactivity than ash thermally treated at 900 °C. From their experiment, ash passing a 90 μm standard sieve facilitated filler and nucleation site effect in the cementitious matrix. To improve the workability of the HPC specimens, a Masterglenium Sky 504 – a polycarboxylic ether (PCE) polymer-based superplasticiser supplied by BASF, Lagos, West Africa Limited was sourced and dispensed at a quantity of 2% by weight of binder (b_{wob}) under the manufactures' details. A thermoset polymer and strictly covalently cross-linked polymer of acrylic acid and acrylamide-based superabsorbent polymers, SAP ("FLOSET 27CC" $\leq$ 300 μm), obtained from bulk solution polymerisation and neutralised by alkaline hydroxide was added to the HPC mixtures as a curing agent. Using the sophisticated quantitative techniques of X-ray fluorescence, XRF (Bruker AXS S4, Explorer, Karlsruhe, Germany), and scanning electron microscope/energy dispersive X-ray, SEM/EDX, (Phenom ProX, PhenomWorld Eindhoven, The Netherlands) the chemical composition and morphology of the BLA were analysed

2.2. Aggregates

This study employed locally sourced river sand as the fine aggregate. The fine aggregate was properly washed to eliminate harmful substances and then sun-dried. The material's quality was further enhanced by removing finer particles that passed through a 300 μm standard sieve. In testing the sand's physical properties, the values for fineness modulus, (FM = 2.78), coefficient of uniformity, (C_u = 2.00), coefficient of curvature, (C_c = 0.20), specific gravity, (SG = 2.65), and water absorption, (0.73%), were determined. The coarse aggregate (granite) larger than 12 mm was sieved out and then thoroughly washed with clean water to remove fine particles. The coarse aggregate had a specific gravity of 2.70, a water absorption rate of 0.52%, and a crushing impact value of 23.13%. The aggregates met the requirements of BS EN 12620:2002: +A1: (2008). These results agreed with and supported the practicability of removing finer sand particles with a 300 μm screen and washing coarse aggregate to lower the dust content (Aitcin, 2004). Fig. 1 displays the particle size distribution (PSD) of the fine and coarse aggregates used in this study. Table 1 further summarises the aggregates' physical attributes. The figure's PSD plot illustrates that the fine aggregate sample conformed to Shetty's (2004) classification of medium sand. The coarse material is uniformly graded. The aggregate results conform to the conditions described in Zeyad et al. (2021a), Zeyad et al. (2021b) and Arulmoly et al. (2021) studies for HPC production.

2.3. Water

The water utilised for this work adhered to the BS EN 1008 (2002) criteria for concrete mixing water.

2.4. HPC specimen proportion

Following the British HPC design technique, the HPC's control sample consists of 515 kg/m^3 of CEM II, 1013.4 kg/m^3 of coarse aggregate, and 675.6 kg/m^3 of fine aggregate, and a total of 155.4 kg/m^3 of water. Based on Olawuyi et al.'s (2021) analysis of the SAP absorbency, 12.5 g/g of water was added. The SAP and superplasticiser concentrations in the combination were maintained at 0.3% and 1.5% b_{wob}, respectively. Other HPC combinations substituted CEM II for BLA in proportions of 5, 10, and 15%, respectively. Binders (CEM II and BLA) and aggregates were weighed separately and mechanically mixed to produce a homogenous mixture. SAP was added and combined with sand and binder mixture in a dry state. To improve the workability of the

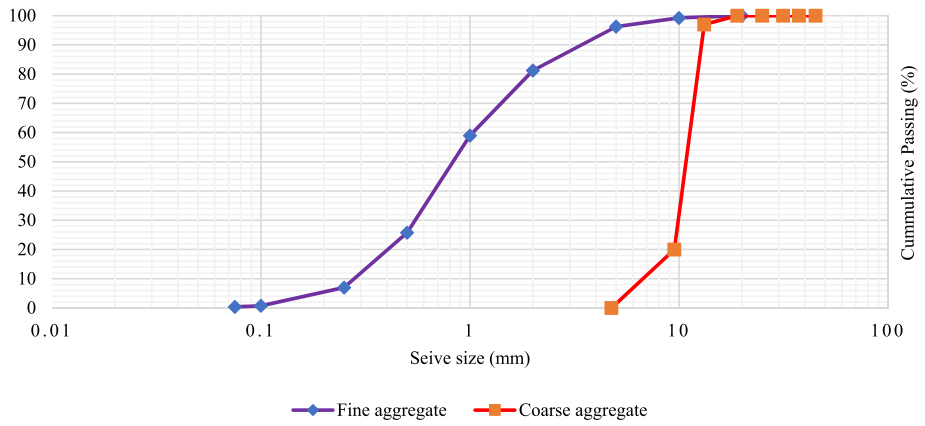

Fig. 1. Particle distribution of aggregates.

Table 1
Physical and mechanical properties of aggregates.

Properties	Sand	Granite
Fineness modulus	2.78	–
Specific gravity	2.65	2.70
Water absorption, %	0.73	0.52
Aggregate crushing value, %	–	23.13
D_{10}, mm	0.5	6.70
D_{30}, mm	0.55	10.00
D_{60}, mm	1.00	10.10
C_u	2.00	1.50
C_c	0.20	5.95

HPC combinations, water containing superplasticiser (Masterglenium Sky 504) was added to the dry HPC mixture after it was thoroughly mixed. The weighted mixing water was divided into two parts and a half was added first before the remaining half mixed with the Masterglenium Sky 504 was added and the mix was allowed to agitate in the mixer for another 3 min. The HPC proportions for the mixtures are given in Table 2. The categories of the HPC were labelled BLAC with BLA content stated. For instance, the HPC containing BLA at a 5% concentration was referred to as BLAC-5.

2.5. HPC casting and curing

For each HPC mixture, 192 numbers of 100 mm cubes were cast for compressive strength, water absorption, and resistance to aggressive chemical environment tests. 48 numbers of 100 Ø x 200 mm cylinders and 46 numbers of 100 x 100 × 500 mm prisms were cast for splitting tensile and flexural strength tests, respectively. In addition, was 16 numbers 100 Ø x 200 mm cylinders cast for the sorptivity test and this was sliced into a 100 Ø x 50 mm disc when dried. The HPC cubes, cylinders, prisms and discs were cast in four BLA contents (i.e. 0%, 5%, 10% and 15%) respectively, and each specimen was allowed to vibrate on a vibrating table for 3 min effective compaction. The specimen was demoulded after 24 h and cured immersed in the various curing media (water, HCl, Na_2SO_4 and $CaCl_2$ solutions) up to the respective curing age (7, 21, 28, and 60 days).

Table 2
HPC mix proportions.

Materials	Mix ID (kg/m^3)			
	Control	BLAC-5	BLAC-10	BLAC-15
Cement (CEM II)	515	515	515	515
BLA	0	1.254	2.508	3.762
Coarse aggrgate	1013	1013	1013	1013
Fine aggregate	676	676	676	676
SAP (0.3% b_{wob})	1.545	1.545	1.545	1.545
Superplasticizer (1.5% b_{wob})	7.725	7.725	7.725	7.725
Water	154.5	154.5	154.5	154.5
Additional Water	0.941	0.941	0.941	0.941
Water/binder (W/B)	0.3	0.3	0.3	0.3

2.6. Testing procedure

2.6.1. Workability

Slump flow of the fresh HPC was performed using the flow table test illustrated in BS EN 12350-5 (2009) as a gauge for the HPC mixtures' workability.

2.6.2. Compressive strength

At ages 7, 21, 28, and 60 days, the compressive strength of the 48-number HPC specimen was evaluated under BS EN 12390-3 (2019) specifications. This was by applying a crushing force on the 100 mm cube specimen through the YES-2000 digital Materials Testing Machine with a maximum loading capacity of 2000 kN ensuring the cast face is placed horizontally to the loading platen. The compressive strength (f_c) is calculated using Eq. (1):

$$f_c = \frac{F}{Ac} \tag{1}$$

where f_c is the compressive strength of the HPC mixture, MPa; F is the maximum load at failure, kN; Ac is the specimen's cross-sectional area, mm.

2.6.3. Splitting tensile strength

The test specimen consisted of 100 Ø x 200 mm cylinders following BS EN 12390-6 (2019) specification. Consequently, 48 number cylinders were examined at ages 7, 21, 28, and 60 days using the linear elastic theory stated in Eq. (2):

$$\sigma_t = \frac{2P}{\pi DL} \tag{2}$$

where σ_t is the splitting tensile strength of the HPC mixture, MPa; P is the failure load, kN; D is the diameter of the specimen, mm, and L is the length of the specimen, mm. YES-2000 digital Materials Testing Machine as in the compressive strength test was utilised for the test with the cylindrical specimen placed lying longitudinally on the platen. The fracture line on the surface of the specimen was initially established by applying diametric compression. The specimen was then positioned in the centre of the pressure plate, with its split line aligned with the centre line at the bottom of the pressure plate.

2.6.4. Flexural strength test

Using a manually operated three-point contact 50 kN Impact AO 320

flexural machine, the flexural strength (also known as the modulus of rupture, MR) of 48 HPC prismatic samples measuring 100 × 100 × 500 mm were evaluated. In the flexural strength test, the test configuration followed BS EN 12390-5 (2019) with the same variables as detailed in the splitting tensile test. As indicated in Equation (3), flexural strength is represented by the modulus of rupture (MR), as shown in Eq. (3).

$$MR = \frac{PL}{bd^2} \quad (3)$$

MR is the modulus of the rapture of the HPC mixture, MPa; P is the failure load, kN; L is the length of the specimen, mm; b is the specimen's breath, and d is the depth of the specimen, mm.

2.6.5. Water absorption test

This study determined the HPC specimen water absorption following BS EN 1097-6 (2013) on 100 concrete cubes cured by immersion in a water tank for 7, 21, 28, and 60 days. The weight of the soaked HPC specimens was initially determined and labelled as M_{wet}; they were subsequently oven-dried at 110 ± 5 °C in a triplex for 24 h until their mass was constant. The dry samples were allowed to cool before being computed and recorded with the designation M_{dry}. The water absorption value was calculated by subtracting the dry sample's mass from the wet sample's mass, dividing the result by the mass of the dry sample, and multiplying the result by 100. The value of water absorption (WA) can be stated mathematically as follows:

$$WA = \frac{Mwet - Mdry}{Mdry} \times 100 \quad (4)$$

WA (%) is the water absorption value; M_{wet} is the wet sample's weight; M_{dry} is the dry sample's weight.

2.6.6. Sorptivity test

To determine the sorptivity coefficient of the HPC samples, capillary water absorption (sorptivity) measurements were performed in accordance with ASTM C 1585-04 (2007) on 100 Ø x 50 mm discs cured in a water tank for 7, 21, 28, and 60 days. After demoulding, specimens were cut from the 100 Ø x 200 mm cylinder using an electric handheld cutting machine. Three-disc samples were weighed and then placed in an oven at 110 ± 5 °C for 24 h for each HPC mixture until a steady weight was achieved. The discs were reweighed to establish a uniaxial water flow, and the circumference was sealed with plastic tape, but the opposing faces were left exposed. The specimen were then stored in a rectangular container filled to 30 mm height with water for approximately 7 h. 5, 10, 15, 30, 60, 120, and 180 min later, the data were recorded to estimate the water absorbed. The samples were then removed and weighed once more to estimate the water absorbed. Eq. (5) was used to compute the results:

$$I = S.t^{0.5} \quad (5)$$

I is the accumulative ingress of water in mm, S is the sorptivity coefficient, and t (min) is the sample's immersion period in the water. The sample's water absorption was converted to volume. The volume of water plotted against the square root of time generates a straight line. By computing the slope of this straight line, the coefficient of sorptivity was obtained. The best-fitting line was then determined using a regression analysis of the data points for every HPC mixture. This mixture's absorption rate corresponded to the slope of the best-fitting line.

2.6.7. Resistance to aggressive chemical environment test

This study used 5% hydrochloric acid (HCl) as an acidic curing environment to assess resistance to acid attack. So also, were, 5% calcium chloride ($CaCl_2$) and sodium sulphate (Na_2SO_4) solutions were utilised to determine the chloride and sulphate resistances of the HPC samples. The 100 mm cubic samples for four mix designs in triplicates were deposited in 5% HCl, 5% $CaCl_2$, and Na_2SO_4 blends for 60 days. Open plastic containers were used while the acid, sulphate and chloride environments' pH was checked during the experimenting cycle. After 30 days, the pH of the solutions was reaffirmed, and the concentration changed. The samples were removed at 7, 21, 28 and 60 days after being exposed to acid, chloride, and sulphate solutions and then rinsed with water. The samples were sun-dried quickly, and the adhering particles were wiped away using a cotton napkin. The influence of acid, chloride and sulphate attack was evaluated using the same compressive testing machine described in section 2.6.3 to measure compressive strength. HPC's cube compressive strength determination followed BS EN 12390-3 (2019) specifications.

2.7. Statistical analysis

The SPSS software version 23 was used to analyse the experiment's findings. The statistical significance between the study's dependent and independent variables was determined using the general linear model - multivariate analysis for the Tests of Between-Subjects Effects. The study had curing age and BLA content as the independent variables, but slump flow, density, compressive strength in water, splitting tensile strength in water, flexural strength in water, water absorption, compressive strength in HCL, compressive strength in Na_2SO_4 and compressive strength in a chlorine solution were all dependent variables.

3. Results

3.1. Characterisation of materials and fresh property

3.1.1. Chemical and microstructure analyses of BLA

3.1.1.1. X-ray fluorescence analysis (XRF). The chemical compositions of BLA used for the blended cement in this study are presented in Table 3. The findings show that BLA calcined at a maximum temperature of 600 °C contains high silica content of 75.1%, calcium oxide of 4.22%, alumina of 3.55% and ferrite of 1.34%. This result confirms that the analysed BLA is a pozzolanic material in consonance with ASTM C 618 (2019) standard provisions. This BLA can be rated under Class F pozzolans since the sum of the percentage elemental oxide content of SiO_2+Al_20_3+Fe_2O_3 equals 80.03%, and higher than the minimum of 70% requirements of ASTM C 618 (2019). As stipulated by the standard, the XRF result also highlights less than 4% of sulfur trioxide (SO_3) composition (1.69%). The loss on ignition (LOI) of 5.32% found on the BLA sample is within the threshold permitted by ASTM C 618 (2019) for pozzolanic materials. Thus, this study's useful oxides (SiO_2+Al_2O_3+Fe_2O_3) and LOI are consistent with the current literature and standards (Olutoge and Oladunmoye, 2017; Kolawole et al., 2021; Silva et al., 2021; Odeyemi et al., 2022; ASTM C 618, 2019) on BLA composition.

3.1.1.2. Scanning electron microscope (SEM) analysis of BLA. The BLA morphology and semi-quantitative chemical elements were analysed using SEM/EDX techniques. Figs. 2 and 3 illustrate the BLA SEM micrograph under 100 μm magnification and EDX peak results. Also, Table 4 highlights the atomic and weight concentrations of the same material. Similar to Silva et al.'s (2021) BLA SEM image of Brazilian origin, this sample's SEM images depict flaky irregular, angular, and needle-like particles denoted as A, B and C interconnected. Also, the SEM image revealed very dark and light grey irregular colours with very dark colours in between them. The very dark colours can be inferred as the air spaces depicting porous materials which ought to enhance easy passages of water for dilution of the cementitious materials and hence improved hydration. The EDX spectra show silica in high content, followed by peaks of potassium and calcium. There are aluminium and iron in low contents in the investigated BLA sample. Thus, silica enrichment in the BLA sample is similar to the result of the chemical oxides.

Table 3
Chemical composition of BLA.

Elemental Oxides	SiO_2	Al_2O_3	Fe_2O_3	CaO	MgO	SO_3	Mn_2O_3	P_2O_5	TiO_2	LOI	SiO_2+Al_2O3+Fe_2O_3
Composition (%)	75.10	3.55	1.34	4.22	4.04	1.69	0.22	1.51	0.26	5. 32	80.03

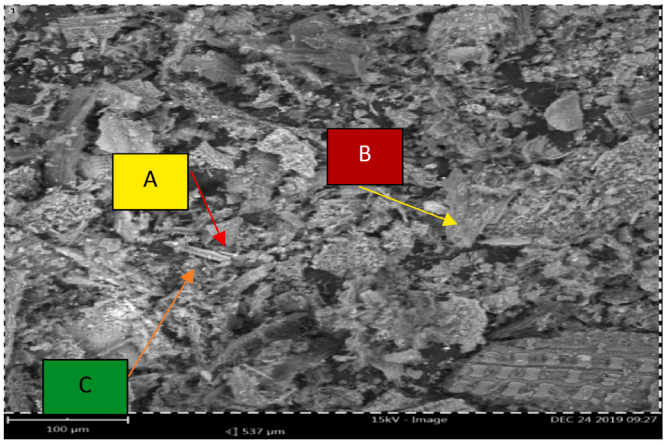

Fig. 2. SEM micrograph of BLA.

3.2. Fresh properties: slump flow test

Fresh HPC mixtures were evaluated for workability using a slump flow test before being cast into moulds. Fig. 4 displays the slump flow tests performed on HPC mixes containing BLA.

From Fig. 4, the slump flow value is influenced greatly by the cement substitution with BLA. The slump flow was less affected by the volume of water and other constituents used, unlike the BLA, which was used to replace cement in the mixture. The result depicts that BLA-15 with 15% PC replacement has the highest slump flow value of 510 mm, followed by the BLAC-10 with a slump flow of 477 mm. BLAC-5 and control mixtures recorded 460 mm and 430 mm slump flow values, respectively. These results indicate that the fresh BLA-based HPC matrix increases workability with higher BLA contents. This scenario may be linked to the BLA's pore structure noticed in the SEM result. The BLAC-15 increases the slump flow value by 18.61% compared to the control alluding to the BLA's capacity to take up the Masterglenium Sky, 504 superplasticiser applied in the mixtures triggering the dispersal and water acceptance propensities (Pang et al., 2022) impacting BLA-based HPC. The improvement in slump flow value between BLAC-15 and the control was attributable to the BLA's capacity to encapsulate the aggregate particles, producing a higher viscosity and enabling the aggregate to flow more readily and with less friction on each other. In addition, BLA's ability to act as a filler enables it to replace the water-filled spaces surrounding aggregate particles, resulting in increased free water, less friction, and improved workability. The findings here are at variance with the slump cone test behaviours of BLA-based concrete investigated by Onikeku et al. (2019) and Abebaw et al. (2021). Onikeku et al. (2019) and Abebaw et al. (2021) studies focused on normal-strength concrete using a slump cone test for workability determination. However, the fluidity

Table 4
EDX atomic and weight concentrations of BLA.

Element Number	Element Symbol	Element Name	Atomic Conc.	Weight Conc.
14	Si	Silicon	38.48	39.18
19	K	Potassium	11.49	16.29
20	Ca	Calcium	10.59	15.39
6	C	Carbon	25.48	11.09
26	Fe	Iron	1.76	3.55
17	Cl	Chlorine	2.54	3.26
15	P	Phosphorus	2.14	2.41
47	Ag	Silver	0.61	2.39
16	S	Sulfur	1.62	1.88
13	Al	Aluminium	1.89	1.85
22	Ti	Titanium	0.45	0.78
12	Mg	Magnesium	0.83	0.73
7	N	Nitrogen	1.09	0.56
8	O	Oxygen	0.86	0.50
11	Na	Sodium	0.17	0.15

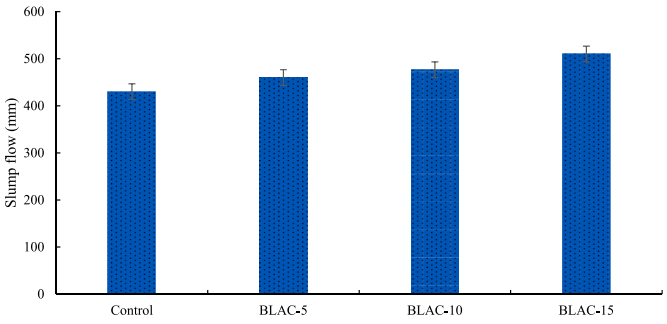

Fig. 4. Slump flow values of different HPC mix designs.

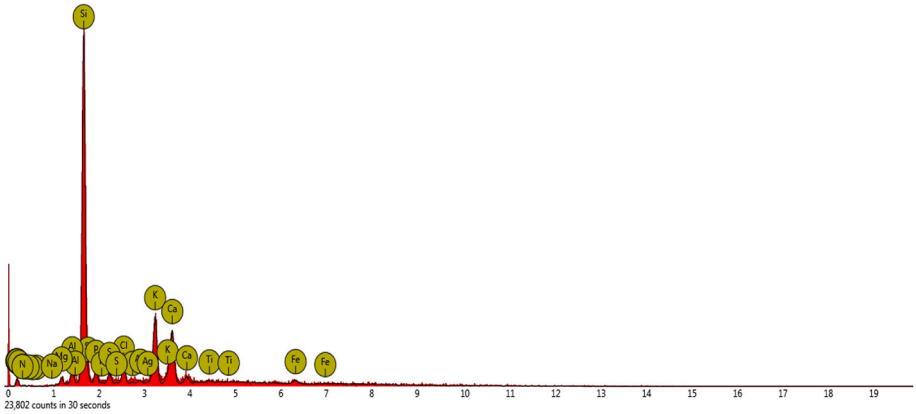

Fig. 3. EDX microanalysis of BLA

values in the current study are consistent with the HPC mixtures in the literature, with a flow range of 400 to 600 mm (Neville, 2012; Nduka et al., 2021).

3.3. Mechanical properties of hardened HPC

3.3.1. Density of HPC

Using Equation (6), the average densities of each HPC sample were calculated, and the values determined from the average of triplicate samples are presented in Fig. 5.

$$\text{density} = \frac{\text{Mass}}{\text{Volume}} \tag{6}$$

From the cylinder samples in Fig. 5, all BLA percentage replacements were slightly lower than the control in the order of replacement, such that BLAC-5 was less by 0.99%, and BLAC-10 was 0.98% lower than the control. From these findings, the reduction of the densities of BLA-based HPC specimens may come from a lower specific gravity of BLA than cement. Aprianti et al. (2015) found BLA's specific gravity and surface area to be 1.9–2.4 and 274 - 943 cm^3/g, respectively. These BLA's physical properties are lower than cement 3.1–3.16 specific gravity and 3100 - 2250 cm^2/gm specific surface area.

3.3.2. Compressive strength of HPC with BLA

Fig. 6 depicts the compressive strength values of HPC cubes combined with BLA at ages 7, 21, 28, and 60 days. The compressive strength improves as the cubes age.

Based on the figure, the compressive strength values in the 7, 21, 28 and 60 days of curing had an increasing trend in all curing regimes. This same trend was reported by Odeyemi et al. (2022) in HPC containing BLA. There was a strength improvement of 2.68% and 1.69%, respectively for BLAC-10 at 21 and 60 days hydration period. The results revealed that the control mixture achieved a compressive strength value of 34.64 MPa, while BLAC-5, BLAC-10, and BLAC-15 achieved compressive strength values of 34.60, 32.35, and 29.94 MPa, respectively at 7 days of curing. At 21 days of curing, the compressive strength results indicate that BLAC-10 has the highest compressive strength value of 47.56 MPa, followed by control with a compressive strength of 46.32 MPa, BLAC-5 with 45.89 MPa, and BLAC-15 with 36.47 MPa least value. At 28 days of curing, control had the highest compressive strength value of 52.05 MPa, then BLAC-10 with 51.08 MPa, followed by BLAC-5 with 49.76 MPa, and lastly BLAC-15 with 43.87 MPa. The findings show that the increase in the percentage of BLA replacement decreases the compressive strength of the specimen, especially at an early age. Thus, BLAC-10 at 28 days attained 51.08 MPa, slightly above the designed characteristics strength of 50 MPa, while 60 days of curing produced a 1.69% increase in compressive strength compared with the control. Also, the present result is at variance with Odeyemi et al. (2022), who obtained 57.59 MPa optimum compressive strength value in BLA-blended HPC at 5% cement replacement. A major shift between the present study and Odeyemi et al. (2022) may be attributed to different designed strength characteristics and target mean strengths.

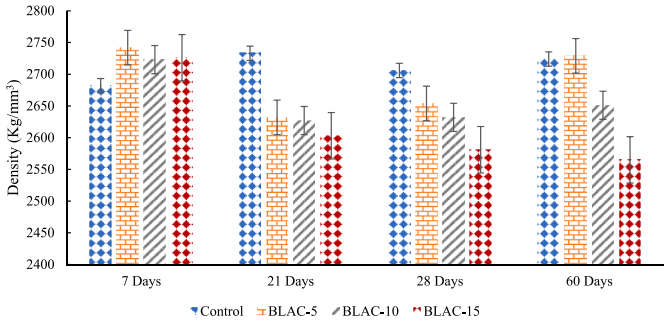

Fig. 5. Densities of BLA-based HPC in 100 Ø x 200 mm cylinder mould.

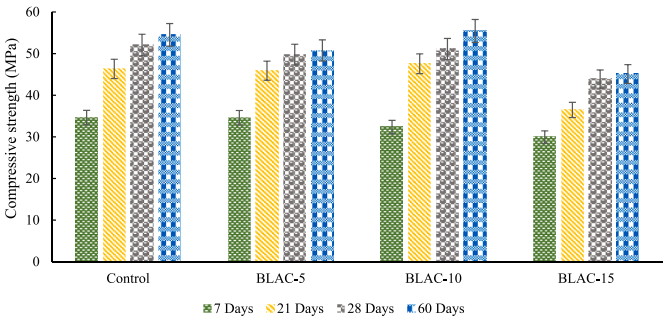

Fig. 6. Compressive strength of BLA-based HPC.

3.3.3. Splitting tensile strength of HPC with BLA

Fig. 7 depicts the splitting tensile strength of HPC cylinders blended with BLA at curing ages 7, 21, 28, and 60 days. The splitting tensile strength of HPC specimens increases as the number of curing days increases but decreases as BLA replacement increases.

As the BLA proportion increased, there was a progressive increase in the splitting tensile strength at 7 days. The BLAC-10 mixture had the highest splitting tensile strength of 3.86 MPa, followed by the control with a value of 3.72 MPa. BLAC-15 and BLAC-5 had a splitting tensile strength of 3.56 and 3.41 MPa. The splitting tensile strength value of BLAC-10 (5.917 MPa) dropped after 21 days of curing, making it the second-highest value to control with a splitting tensile strength of 6.06 MPa. The BLAC-5 mixture's splitting tensile strength value was 5.67 MPa, and the BLAC-15 with a value of 4.62 MPa. At 28 days of curing, the control mixture still retains the highest splitting tensile strength value of 7.35 MPa, while BLAC-5 recorded a 6.76 MPa showing an improvement after 7 and 21 days of curing. BLAC-10 mixture demonstrated a splitting tensile strength value of 6.13 MPa, while BLAC-15 shows the least splitting tensile strength value of 5.52 MPa. At 60 days, control still possesses the highest splitting tensile strength value of 8.54 MPa, followed by BLAC-10 with 7.99 MPa. Thus, the splitting tensile strength values are consistent with the compressive strength values reinforcing the amorphous characteristics of BLA in the cementitious matrix (Thomas et al., 2021).

3.3.4. Flexural strength of HPC with BLA

Fig. 8 depicts the flexural strength study of HPC prisms blended with varying percentages of BLA substitution. Similar to the compressive strength and splitting tensile strength values, the data demonstrate that flexural strength increases with increasing age.

As shown in the Figure, at 7 days of curing, BLAC-10 recorded the maximum flexural strength value of 1.15 MPa, followed by BLAC-5 with a flexural strength of 1.12 MPa. BLAC-5 and BLAC-10 showed a significant improvement after 7 days of curing. The flexural strength value of 1.00 MPa was obtained for the control at the same age, while BLAC-15 had the least flexural strength value of 0.87 MPa. Similar to 7 days curing results, BLAC-10 remained the most improved mixture recording 1.23 MPa at 21 days, next is the BLAC-5 with 1.20 MPa. The flexural strength values of control and BLAC-15 were 1.12 and 1.10 MPa, respectively, after 28 days of curing. For the 60 days of curing, BLAC-10 had a flexural strength of 1.76 MPa, followed by control with 1.73 MPa. BLAC-5 had a strength value of 1.67 MPa, and the least flexural strength value for 60 days of curing is BLAC-15, with a strength of 1.32 MPa. The increased flexural strength observed in the BLA-blended mixture, especially with the BLA-10 mixture, may be attributed to the high SiO_2 values revealed in the XRF and EDX micrograph and atomic and weight concentration results of the tested BLA. The SiO_2 content in BLA influences pozzolanic reactivity in cementitious products (Silva et al., 2021). The finding here complied with both compressive and splitting tensile test results.

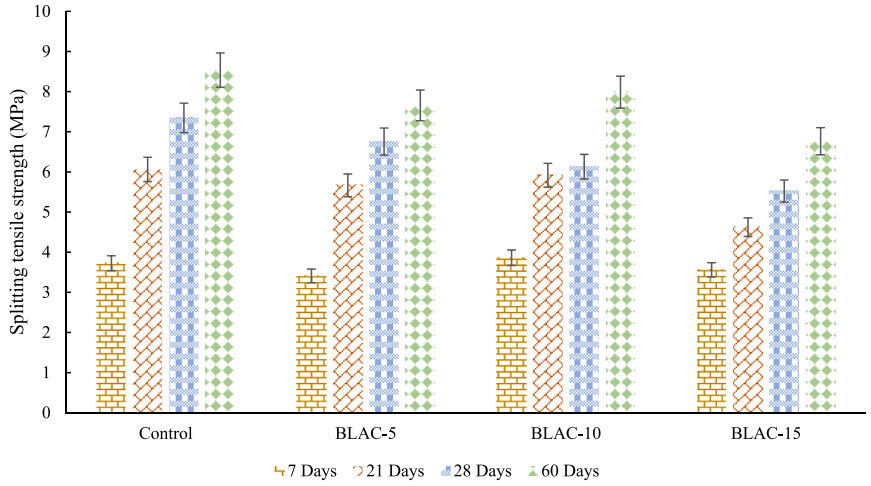

Fig. 7. Splitting tensile strength of BLA-based HPC.

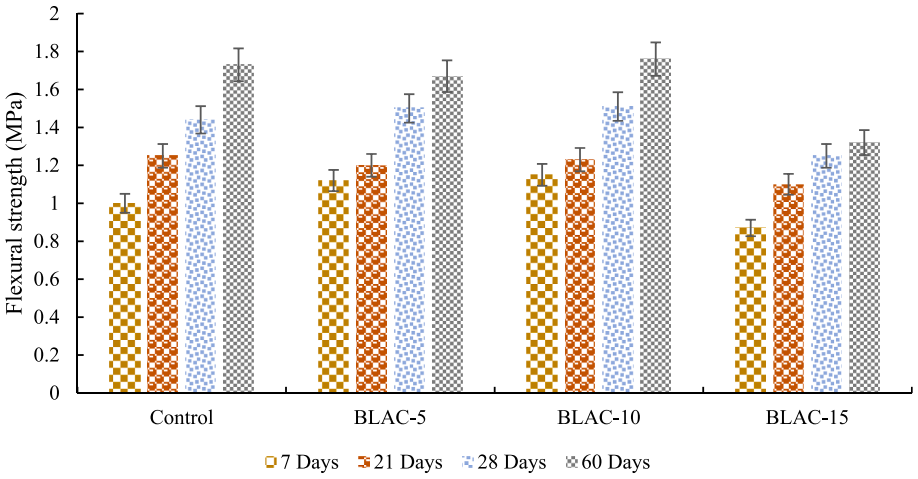

Fig. 8. Flexural strength of BLA-based HPC.

3.4. Durability properties

3.4.1. Water absorption of HPC

Fig. 9 shows the mean experimental results for the water absorption of BLA-modified HPCs at 7, 21, 28, and 60 days. The water absorption varied from 5.10 to 7.10% for 7 days, 5.01 to 7.02% for 21 days, 4.19 to 6.96% for 28 days, and 4.07 to 6.79% for 60 days. The control mixture without BLA complied with ASTM C 642 (2006) provisions with an acceptable range of 2–5% water absorption for HPC mixtures. On the other hand, BLA blended HPCs had water absorption values slightly

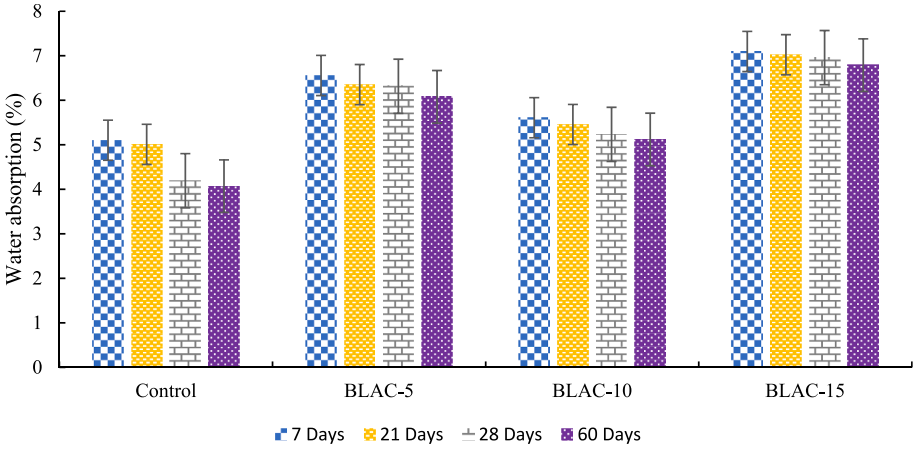

Fig. 9. Water absorption of BLA-based HPC at various curing days.

higher than that prescribed by the relevant standard. Silva et al. (2021) reported increased water absorption when more than 10% of PC was replaced with BLA in the mortar mixture. Increased water absorption may be attributable to the mesoporous nature of the tested BLA sample, confirmed by the SEM image. However, the BLAC-10 mixture had the lowest water absorption capacity among the BLA blended HPCs confirming the best-improved mixture in the tested mechanical properties results. For instance, there are 16.90 and 25.05%, 16.42 and 28.72%, 20.63 and 32.94%, and 18.71 and 32.21% water absorption reductions for BLAC-10 compared to the BLAC-5 and BLAC-15 HPCs at 7, 21, 28 and 60 days of curing, respectively. The water absorption values obtained in BLAC-10 mixtures are moderately above 5% at 60 days compared with 28 days, signalling the best-improved mixture among the blends. The decrease in water absorption may indicate the efficacy of BLA particles in densifying the cement paste matrix and the interface between the cement paste and aggregates. Moreover, the creation of calcium silicate and calcium silicate aluminate hydrates (C-S-H and C-A-H) via the pozzolanic activity further fills the pores and enhances the microstructure of the BLA-blended HPC.

3.4.2. Sorptivity of HPCs

The changes in water absorption by capillary pressure as a function of time have been illustrated in Fig. 10 through 13. The absorption rate (sorptivity coefficient) plots for BLA-modified HPCs were analysed in conjunction with the change in mass per unit area relative to the water unit mass and the period's square root (min). The effects of blended BLA on the water sorptivity of HPC at 7, 21, 28, and 60 days are depicted in Figs. 10-13. During the seven days of curing, the capillary water activity of BLAC-10 (1.87 mm) dropped the most compared to the control (2.75 mm) and other combinations. Also, a 28-day BLAC-10 had the lowest water capillary ingress of approximately 0.74–4.50 mm over the 180 min inspection time compared with other mixes. The BLAC-10 mixture had a mean water sorptivity of 2.12 mm to the control mix (2.62 mm). A related trend was observed at 60 days; the mean water ingress was 2.30 mm for the BLAC-10 modified HPC.

The correlation coefficient of BLA-based HPC at 7, 21, 28 and 60 days is shown in Table 5. On all curing days of 7, 21, 28, and 60 days, the control mixture demonstrated a good correlation between the rate of absorption and the square root of time, with $R^2 = 0.966$ (7 days), 0.979 (21 days), 0.964 (28 days) and 0.911 (60 days), respectively. These results demonstrate the hydration trends of the examined samples as curing days progressed. The correlation coefficients for BLAC-5 were $R^2 = 0.997$ (7 days), 0.944 (21 days), 0.985 (28 days) and 0.948 (60 days), respectively. For BLAC-10, the correlation coefficients recorded were $R^2 = 0.994$ (7 days), 0.990 (21 days), 0.983 (28 days) and 0.980 (60 days), respectively. Lastly, BLAC-15 had correlation coefficients of $R^2 = 0.987$ (7 days), 0.988 (21 days), 0.995 (28 days) and 0.995 (60 days), respectively. ASTM C 1585-04 (2007) guideline stated, "The initial absorption rate cannot be established if the data between 1 min and 6 h do not follow a linear connection (correlation coefficient less than 0.98) and exhibit a systematic curvature." Thus, the BLAC-5 correlation coefficient was significant at 21, 28 and 56 days but not at 7 days. BLAC-10 revealed a significant difference at 28 and 56 days, but BLAC-15 gave differences in the calculated correlation coefficient between 7, 21, 28, and 60 days.

3.4.3. Resistance to the aggressive chemical environment

Figs. 14-17 depict the compressive strength at 7, 21, 28, and 60 days of hardened HPCs with varied PC substitutions by BLA subjected to various curing media (water, acid, sulphate, and chlorine solutions). According to the data, the compressive strength of the HPCs in aggressive environments decreased by 8.40, 27.68, 40.86, and 46.34% (acid); 22.63, 38.64, 47.72, and 51.13% (sulphate) and 14.81, 41.45, 52.80, and 43.46% (chlorine) after 7, 21, 28, and 60 days of curing, respectively, in comparison to curing in water. The sulphate environment strongly influenced the investigated samples' compressive strength for all the mix types. Comparing the plain water curing of HPCs with other chemical environments, the control had the least reduced compressive strength percentage (30.82%), followed by BLAC-15 (31.49%), while the other mixture's compressive strength reduction was within 40.14%. In the sulphate solution, BLAC-5 had the least strength reduction (37.27%), then control (40.04%), while the other mixture's strength reduction was 46.90%. Similarly, BLAC-10 has the lowest strength reduction (34.92%), while other HPC mixtures' strength reduction was 45.42%. In general, the control mixture demonstrated superior reductions in compressive strength in the tested chemical conditions. Therefore, it can be inferred that mesoporous BLA particles produced pores in the HPCs, allowing acid, sulphate, and chloride ions to enter the matrix. The findings complied with the water absorption and sorptivity results in the HPC matrix water ingress.

3.5. Statistical analysis

Table A in the appendix shows the general linear model – multivariate analysis for the Tests of Between-Subjects Effects obtained by SPSS v 23 highlighting the effects of BLA content, and curing age on the compressive, splitting tensile and flexural strengths, slump flows, density, water absorption, compressive strength in acid, sodium sulphate and chloride solutions curing environments of BLA-based HPC mixtures. The significance is assessed based on $P < 0.5$ (as shown in the last column of the Table). The results show that each independent variable (BLA content and curing age) had a significant effect on all the tested properties of the HPC mixtures except the slump flow values which were purely for an assessment of workability done only at the fresh state of the

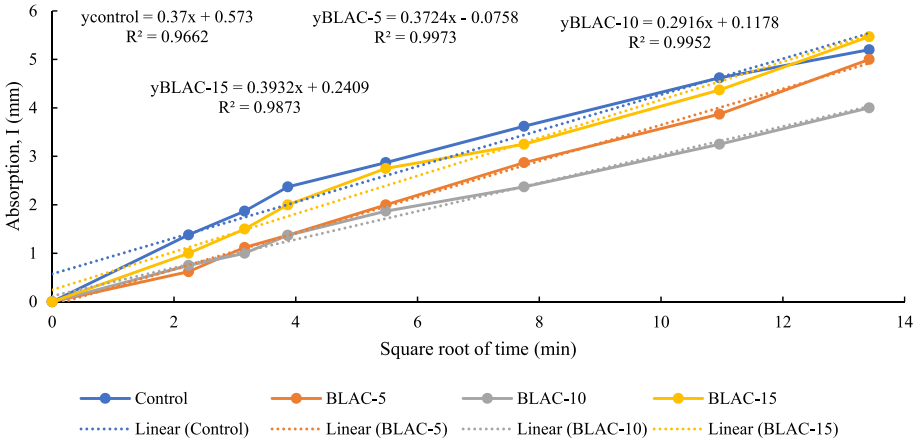

Fig. 10. Water sorptivity characteristics of BLA-blended HPC for 7 days.

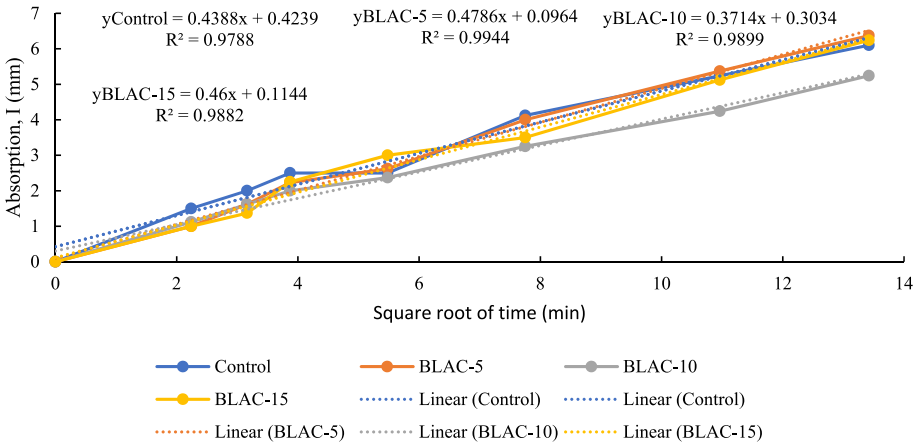

Fig. 11. Water sorptivity characteristics of BLA-blended HPC for 21 days.

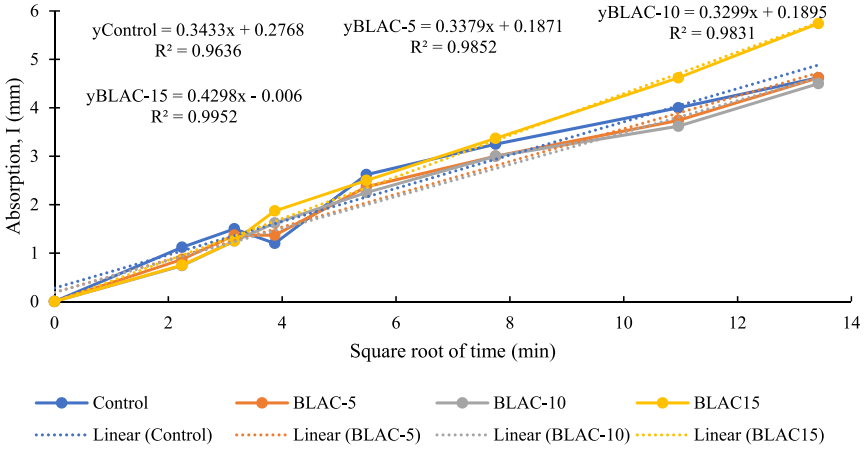

Fig. 12. Water sorptivity characteristics of BLA-blended HPC for 28 days.

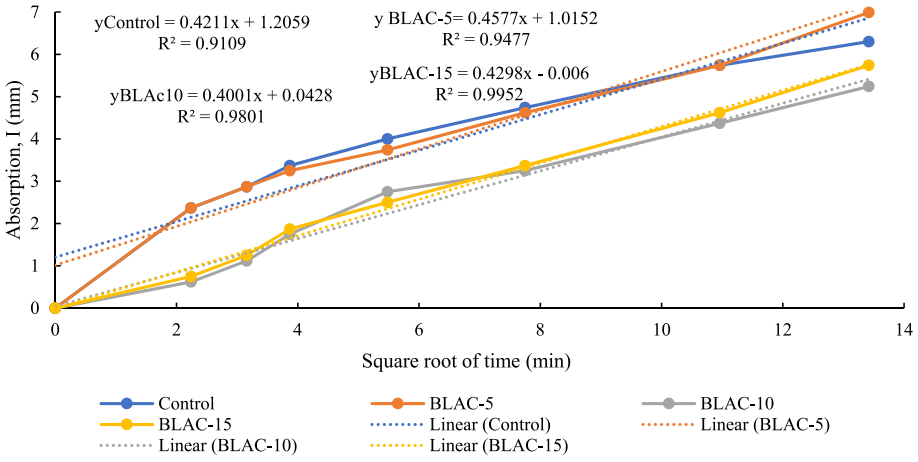

Fig. 13. Water sorptivity characteristics of BLA-blended HPC for 60 days.

concrete. The slump flow value was not influenced by curing age since it was determined before the concrete was cast, so the same slump flow value holds for all curing ages considered. This explains the P value of 1.0 gotten as an outcome of the analysis for the single-factor analysis with curing age and also, the two-factor analysis (Curing Age combined with BLA content) affirming the curing age has no significant effect on slump flow. The variable of influence on the slump flow is the BLA content. Generally, both the curing age and BLA content were observed to have a very strong influence (with a P value of 0.00) on all the tested mechanical and durability properties of the investigated BLA-modified HPC.

Table 5
Summary of water sorptivity correlation coefficient of BLA-blended HPCs.

Mix ID/Sorptivity correlation coefficient	7 days	21 days	28 days	60 days
	R^2	R^2	R^2	R^2
Control	0.966	0.979	0.964	0.911
BLAC-5	0.997	0.944	0.985	0.948
BLAC-10	0.994	0.990	0.983	0.980
BLAC-15	0.987	0.988	0.995	0.995

4. Conclusions

By building upon the scientific contributions of past studies on the use of SCMs as a substitute in cementitious products, the present paper identified the feasibility of the blend of BLA and PC for HPC development. Thus, this experimental study investigated the mechanical and durability properties of BLA-based HPC to establish their relevance for structural element works. Using standard testing procedures, the study found that the analysed BLA falls under the Class F pozzolans of ASTM C 618 (2015) classification ($Si0_2+Al_20_3+Fe_20_3$ = 80.03%), with SEM image showing flaky irregular, angular and needle-like particles affirming the BLA sample as an amorphous material. BLA content has a significant influence on the workability of the HPC mixtures deducing from the slump flow increases from BLA contents increases. PC substitution with BLA in HPC accounted for reduced density in the tested samples while the optimum BLA content for use in HPC is 10% for acceptable mechanical and durability properties. BLA-modified HPC should not be used in severe acidic, sulphate and chloride environments. Curing age and BLA content had a significant effect on the tested mechanical and durability properties of the investigated BLA-modified HPC. It is the idea of this paper to be used by researchers and construction professionals as one of the inputs for steering new alternative materials in building projects. It will also serve as a source of information for the general public. The present study thereby recommends the adoption of 10% BLA content for the production of HPC exposed to normal environmental conditions.

Funding

There was no external funding for the study.

Compliance with ethical standards

This paper does not contain any studies involving human or animal subjects.

Credit authorship contribution statement

David O. Nduka: Conceptualisation, writing-review & editing. Babatunde J. Olawuyi: Formal analysis and writing-review & editing.

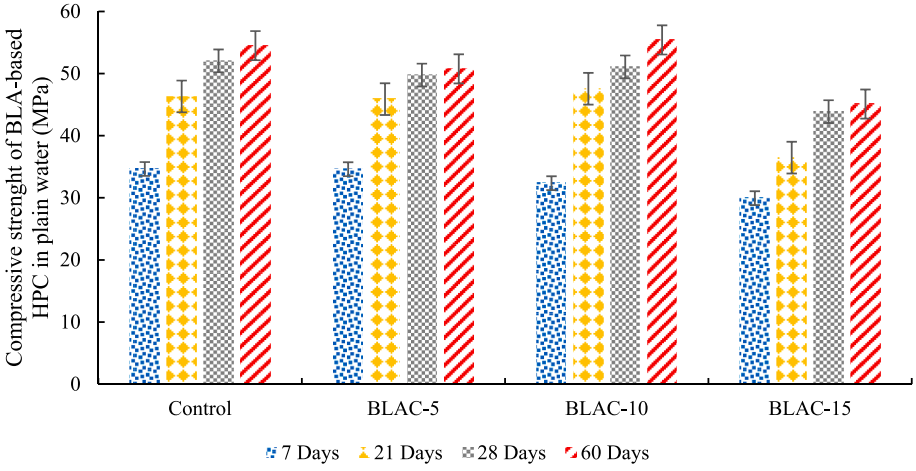

Fig. 14. Compressive strength of BLA-blended HPC cured in a plain water.

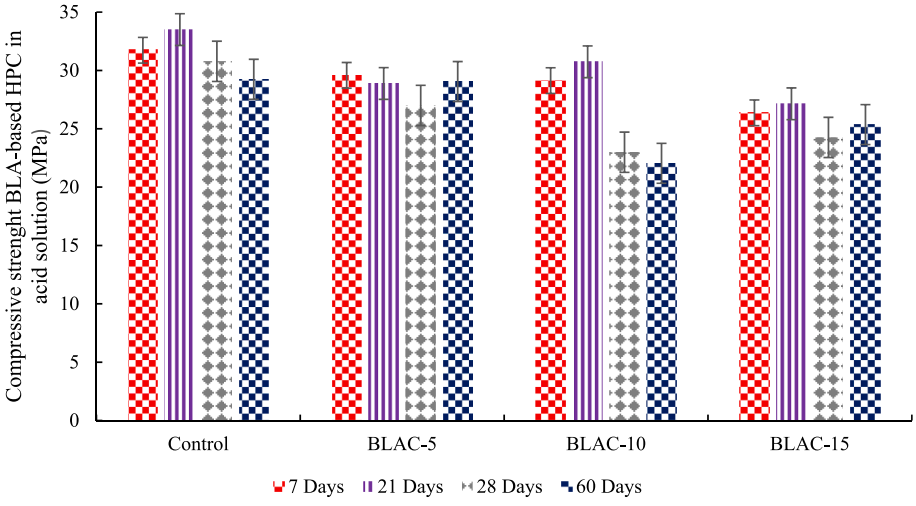

Fig. 15. Compressive strength of BLA-blended HPC cured in an acid environment.

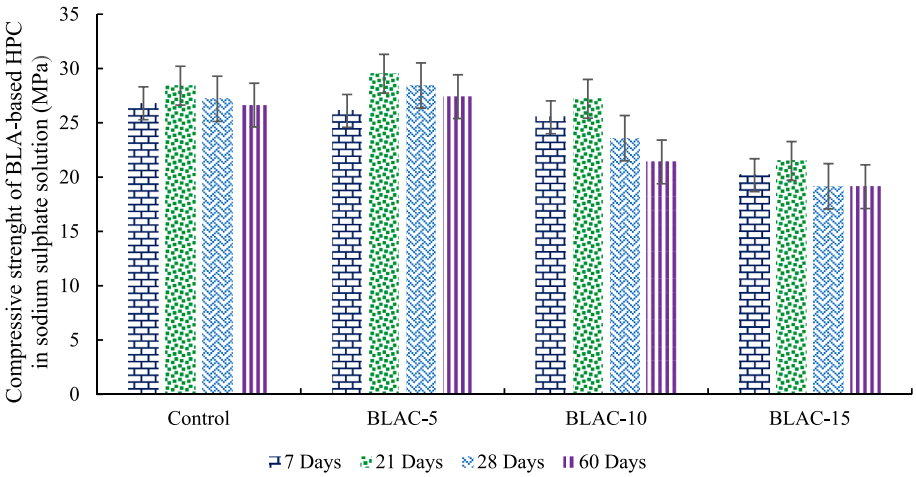

Fig. 16. Compressive strength of BLA-blended HPC cured in a sulphate environment.

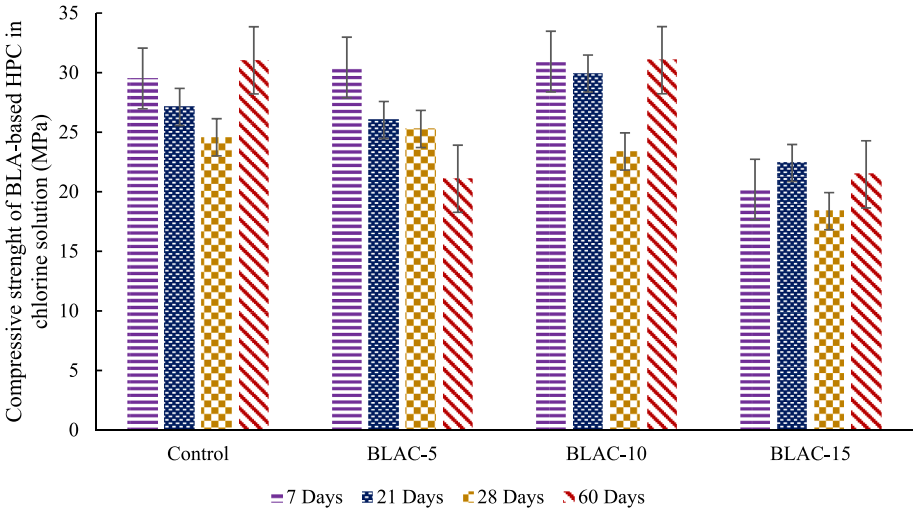

Fig. 17. Compressive strength of BLA-blended HPC cured in a chlorine environment.

Adekunle M. Ajao: Methodology, Project administration. Victor C. Okoye: Writing-original draft, Formal analysis. Obinna M. Okigbo: Writing-original draft, Formal analysis.

Declaration of competing interest

The authors declare that they have no known competing financial interests or personal relationships that could have appeared to influence the work reported in this paper.

Data availability

Data will be made available on request.

Acknowledgement

The authors would like to thank Covenant University for using the laboratory and equipment and sponsoring this paper's article processing charge (APC). Supplier of Masterglenium Sky 504, BASF, Lagos, West Africa, facilitated by Mr Adesola Mofikoya, is acknowledged.

Appendix

Table A
Tests of Between-Subjects Effects of BLA-based HPC on workability, mechanical and durability properties

Source	Dependent Variable	Type III Sum of Squares	df	Mean Square	F	Sig.
Curing Age	Slump flow	.000	3	.000	.000	1.000
	Density	9939.063	3	3313.021	50.420	.000
	Compressive strength in water	2433.734	3	811.245	1.990E3	.000
	Splitting tensile strength in water	106.503	3	35.501	2.031E3	.000
	Flexural strength in water	2.363	3	.788	579.902	.000
	Water Absorption	1.943	3	.648	20.325	.000
	Compressive strength in HCl	134.781	3	44.927	110.155	.000

(*continued on next page*)

Table A (*continued*)

Source	Dependent Variable	Type III Sum of Squares	df	Mean Square	F	Sig.
	Compressive strength in Na_2SO_4	464.875	3	154.958	765.298	.000
	Compressive strength in Chlorine solution	154.703	3	51.568	156.696	.000
BLA content	Slump flow	40100.000	3	13366.667	130.939	.000
	Density	13536.063	3	4512.021	68.667	.000
	Compressive strength in water	496.345	3	165.448	405.811	.000
	Splitting tensile strength in water	10.524	3	3.508	200.657	.000
	Flexural strength in water	.554	3	.185	135.890	.000
	Water Absorption	38.763	3	12.921	405.519	.000
	Compressive strength in HCl	233.169	3	77.723	190.566	.000
	Compressive strength in Na_2SO_4	58.076	3	19.359	95.608	.000
	Compressive strength in a Chlorine solution	494.660	3	164.887	501.033	.000
Curing Age * BLA content	Slump flow	.000	9	.000	.000	1.000
	Density	47980.688	9	5331.188	81.134	.000
	Compressive strength in water	86.942	9	9.660	23.694	.000
	Splitting tensile strength in water	4.258	9	.473	27.062	.000
	Flexural strength in water	.130	9	.014	10.638	.000
	Water Absorption	1.346	9	.150	4.693	.001
	Compressive strength in HCl	89.610	9	9.957	24.412	.000
	Compressive strength in Na_2SO_4	34.474	9	3.830	18.918	.000
	Compressive strength in a Chlorine solution	201.348	9	22.372	67.981	.000

References

Abebaw, G., Bewket, B., Getahun, S., 2021. Experimental investigation on effect of partial replacement of cement with bamboo leaf ash on concrete property. Adv. Civ. Eng. 2021 https://doi.org/10.1155/2021/6468444.

AciTHPC/TAC, 1999. *ACI Defines High-Performance Concrete* (The Technical Activities Committee Report. Chairman - H.G. Russell. American Concrete Institute, USA.

Aïtcin, P.C., 2004. High-Performance Concrete. Taylor & Francis e-Library, New York, NY, USA. Available online: https://books.google.com.ng/books?hl=en&lr=&id=d_yojcvXOf4C&oi=fnd&pg=PP1&dq=12.%09A%C3%AFtcin,+P.+C.+(2004).+High-Performance+Concrete.+Taylor+%26+Francis+e-Lbrary.+New+York,+USA.&ots=JmH4mhbT8X&sig=JekjYus5gV7zw4VwmukejXu0O4Q&redir_esc=y#v=onepage&q&f=false. (Accessed 20 November 2021).

Aprianti, E., Shafigh, P., Bahri, S., Farahani, J.N., 2015. Supplementary cementitious materials origin from agricultural wastes–A review. Construct. Build. Mater. 74, 176–187. https://doi.org/10.1016/j.conbuildmat.2014.10.010.

ASTM C618, 2019. Standard Specification for Coal Fly Ash and Raw or Calcined Natural Pozzolan for Use in Concrete. ASTM International, West Conshohocken, PA, USA.

Arulmoly, B., Konthesingha, C., Nanayakkara, A., 2021. Performance evaluation of cement mortar produced with manufactured sand and offshore sand as alternatives for river sand. Construction and Building Materials 297. https://doi.org/10.1016/j.conbuildmat.2021.123784.

ASTM C642, 2006. Density, Absorption, and Voids in Hardened Concrete. ASTM International, Pennsylvania, USA.

ASTM C1585-04, 2007. Standard Test Method for Measurement of Rate of Absorption of Water by Hydraulic-Cement Concretes. ASTM International, West Conshohocken, PA. USA.

BS EN 197-1, 2011. Cement, Composition, Specifications and Conformity Criteria for Common Cements. British Standard Institution (BSI), London, England.

BS EN 1008, 2002. Mixing Water for Concrete: Specification for Sampling, Testing and Assessing the Suitability of Water, Including Water Recovered from Processes in the Concrete Industry as Mixing Water for Concrete. British Standards Institution, London, UK. Available online: https://standards.iteh.ai/catalog/standards/cen/8ab1a0fa-b727-48f7-9b31-739eba3732ca/en-1008-2002.

BS EN 1097-6, 2013. Tests for Mechanical and Physical Properties of Aggregates Part 6: Determination of Particle Density and Water Absorption. B.S.I. Standards Ltd, Brussels, Belgium.

BS EN 12620:2002+A1, 2008. Specification for Aggregates from Natural Sources for Concrete. British Standard Institute, London, UK.

Chinnu, S.N., Minnu, S.N., Bahurudeen, A., Senthilkumar, R., 2021. Reuse of industrial and agricultural by-products as pozzolan and aggregates in lightweight concrete. Construct. Build. Mater. 302, 124172 https://doi.org/10.1016/j.conbuildmat.2021.124172.

Dembovska, L., Bajare, D., Pundiene, I., Vitola, L., 2017. Effect of pozzolanic additives on the strength development of high-performance concrete. Procedia Eng. 172, 202–210. https://doi.org/10.1016/j.proeng.2017.02.050.

Dushimimana, A., Niyonsenga, A.A., Nzamurambaho, F., 2021. A review on strength development of high-performance concrete. Construct. Build. Mater. 307, 124865 https://doi.org/10.1016/j.conbuildmat.2021.124865.

Dwivedia, V.N., Singhb, N.P., Dasa, S.S., Singha, N.B., 2006. A new pozzolanic material for cement industry: bamboo leaf ash. Int. J. Phys. Sci. 1 (3), 106–111. https://doi.org/10.5897/IJPS.9000022.

"BS EN 12390-3, 2019": BS EN 12390-3, 2019. Testing hardened concrete. In: Compressive Strength of Test Specimens. British Standard Institute, London, UK.

"BS EN 12390-3, 2019":BS EN 12390-5, 2019. Testing Hardened Concrete. Flexural Strenght of Test Specimens. British Standards Institution, London, UK.

Frías, M., Savastano, H., Villar, E., de Rojas, M.I.S., Santos, S., 2012. Characterisation and properties of blended cement matrices containing activated bamboo leaf wastes. Cement Concr. Compos. 34 (9), 1019–1023. https://doi.org/10.1016/j.cemconcomp.2012.05.005.

K Al-Chaar, G., Alkadi, M., Asteris, P.G., 2013. Natural pozzolan as a partial substitute for cement in concrete. Open Construct. Build Technol. J. 7 (1) https://doi.org/10.2174/1874836801307010033.

Kasaniya, M., Thomas, M.D., Moffatt, E.G., 2021. Efficiency of natural pozzolans, ground glasses and coal bottom ashes in mitigating sulfate attack and alkali-silica reaction. Cement Concr. Res. 149, 106551 https://doi.org/10.1016/j.cemconres.2021.106551.

Kolawole, J.T., 2015. Durability of Ternary Blended Cement Concrete Containing Bamboo Leaf Ash and Pulverized Burnt Clay. MSc. Thesis, Obafemi Awolowo University, Ile-Ife, Nigeria. Available online: https://scholar.google.com/scholar?hl=en&as_sdt=0%2C5&q=Durability+of+Ternary+Blended+Cement+Concrete+Containing+Bamboo+Leaf+Ash+and+Pulverized+Burnt+Clay+Waste+in+Sulphuric+Acid+Durability+of+Ternary+Blended+Cement+Concrete+in+Sulphuric+Acid&btnG=.

Kolawole, J.T., Olusola, K.O., Babafemi, A.J., Olalusi, O.B., Fanijo, E., 2021. Blended cement binders containing bamboo leaf ash and ground clay brick waste for sustainable concrete. Materialia 15, 101045. https://doi.org/10.1016/j.mtla.2021.101045.

Mehta, P.K., Monteiro, P.J., 2017. Concrete: Microstructure, Properties, and Materials. McGraw-Hill Education, New York. https://d1wqtxts1xzle7.cloudfront.net/60143083/P.K.Metha_CONCRETE_microstructure_properties_and_materials20190728-128677-m0x541.

Mo, K.H., Alengaram, U.J., Jumaat, M.Z., Yap, S.P., Lee, S.C., 2016. Green concrete partially comprised of farming waste residues: a review. J. Clean. Prod. 117, 122–138. https://doi.org/10.1016/j.jclepro.2016.01.022.

Moraes, M.J.B., Moraes, J.C.B., Tashima, M.M., Akasaki, J.L., Soriano, L., Borrachero, M.V., Paya, J., 2019. Production of bamboo leaf ash by auto-combustion for pozzolanic and sustainable use in cementitious matrices. Construct. Build. Mater. 208, 369–380. https://doi.org/10.1016/j.conbuildmat.2019.03.007.

Nduka, D.O., Ameh, J.O., Joshua, O., Ojelabi, R., 2018. Awareness and benefits of self-curing concrete in construction projects: builders and civil engineers perceptions. Buildings 8 (8), 109. https://doi.org/10.3390/buildings8080109.

Nduka, D.O., Olawuyi, B.J., Fagbenle, O.I., Fonteboa, B.G., 2021. Effect of KyAl4 (Si8-y) O20 (OH) 4 calcined based-clay on the microstructure and mechanical performances of high-performance concrete. Crystals 11 (10), 1152. https://doi.org/10.3390/cryst11101152.

Nduka, D.O., Olawuyi, B.J., Joshua, O.O., Omuh, I.O., 2022. A study on gel/space ratio development in binary mixture containing Portland cement and meta-illite calcined clay/rice husk ash. Gels 8 (2), 85. https://doi.org/10.3390/cryst12010075.

Neville, A.M., 2012. Properties of Concrete, fifth ed. Pearson Educational Limited, London, England https://www.pearson.com/uk/educators/higher-education educators/program/Neville-Properties-of-Concrete-Properties-of-Concrete-5th-Edition/PGM1001873.html.

NIS 444-1, 2018. Composition, specification and conformity criteria for common cements. Standards organisation of Nigeria. https://standards.lawnigeria.com/cgi-sys/suspendedpage.cgi.

Odeyemi, S.O., Atoyebi, O.D., Kegbeyale, O.S., Anifowose, M.A., Odeyemi, O.T., Adeniyi, A.G., Orisadare, O.A., 2022. Mechanical properties and microstructure of High-Performance Concrete with bamboo leaf ash as additive. Cleaner Engineering and Technology 6, 100352. https://doi.org/10.1016/j.clet.2021.100352.

Olawuyi, B.J., Babafemi, A.J., Boshoff, W.P., 2021. Early-age and long-term strength development of high-performance concrete with SAP. Construct. Build. Mater. 267, 121798 https://doi.org/10.1016/j.conbuildmat.2020.121798.

Olutoge, F., Oladunmoye, O., 2017. Bamboo leaf ash as supplementary cementitious material. Am. J. Eng. Res 14 (6), 1–8.

Onikeku, O., Shitote, S.M., Mwero, J., Adedeji, A., 2019. Evaluation of characteristics of concrete mixed with bamboo leaf ash. Open Construct. Build Technol. J. 13 (1) https://doi.org/10.2174/1874836801913010067.

Oyebisi, S., Ede, A., Olutoge, F., Omole, D., 2020. Geopolymer concrete incorporating agro-industrial wastes: effects on mechanical properties, microstructural behaviour and mineralogical phases. Construct. Build. Mater. 256, 119390 https://doi.org/10.1016/j.conbuildmat.2020.119390.

Pang, L., Liu, Z., Wang, D., An, M., 2022. Review on the application of supplementary cementitious materials in self-compacting concrete. Crystals 12 (2), 180. https://doi.org/10.3390/cryst12020180.

Rodier, L., Villar-Cociña, E., Ballesteros, J.M., Junior, H.S., 2019. Potential use of sugarcane bagasse and bamboo leaf ashes for elaboration of green cementitious materials. J. Clean. Prod. 231, 54–63. https://doi.org/10.1016/j.jclepro.2019.05.208.

Shetty, M.S., 2004. Concrete technology - theory and practice. In: Midrand, South Africa. S. Chand and Company Limited Technology, New Delhi, India, pp. 219–228. Cement and Concrete Institute.

Silva, L.H.P., Tamashiro, J.R., de Paiva, F.F.G., dos Santos, L.F., Teixeira, S.R., Kinoshita, A., Antunes, P.A., 2021. Bamboo leaf ash for use as mineral addition with Portland cement. J. Build. Eng. https://doi.org/10.1016/j.jobe.2021.102769, 102769.

Thomas, B.S., Yang, J., Mo, K.H., Abdalla, J.A., Hawileh, R.A., Ariyachandra, E., 2021. Biomass ashes from agricultural wastes as supplementary cementitious materials or aggregate replacement in cement/geopolymer concrete: a comprehensive review. J. Build. Eng. 40, 102332 https://doi.org/10.1016/j.jobe.2021.102332.

Villar-Cociña, E., Morales, E.V., Santos, S.F., Savastano Jr., H., Frías, M., 2011. Pozzolanic behavior of bamboo leaf ash: characterisation and determination of the kinetic parameters. Cement Concr. Compos. 33 (1), 68–73. https://doi.org/10.1016/j.cemconcomp.2010.09.003.

Xu, F., Lin, X., Zhou, A., 2021. Performance of internal curing materials in high-performance concrete: a review. Construct. Build. Mater. 311, 125250 https://doi.org/10.1016/j.conbuildmat.2021.125250.

Zeyad, A.M., Johari, M.A.M., Abadel, A., Abutaleb, A., Mijarsh, M.J.A., Almalki, A., 2022. Transport properties of palm oil fuel ash-based high-performance green concrete subjected to steam curing regimes. Case Stud. Constr. Mater. 16, e01077 https://doi.org/10.1016/j.cscm.2022.e01077.

Zeyad, A.M., Johari, M.A.M., Abutaleb, A., Tayeh, B.A., 2021a. The effect of steam curing regimes on the chloride resistance and pore size of high–strength green concrete. Construct. Build. Mater. 280, 122409 https://doi.org/10.1016/j.conbuildmat.2021.122409.

Zeyad, A.M., Johari, M.A.M., Alharbi, Y.R., Abadel, A.A., Amran, Y.M., Tayeh, B.A., Abutaleb, A., 2021b. Influence of steam curing regimes on the properties of ultrafine POFA-based high-strength green concrete. J. Build. Eng. 38, 102204 https://doi.org/10.1016/j.jobe.2021.102204.